

COMPARATIVE NEUTRONIC ANALYSIS OF IRT FUELS

Ramadan M. Kuridan and Ayman M. Dandi

Nuclear Engineering Department,
Al-Fateh University, Tripoli, Libya

المخلص

استخدمت في هذا البحث طريقة مونت كارلو لأجل مقارنة التحليل النيوتروني لثلاثة أنواع من الوقود النووي IRT في أشكال مختلفة من التجميعات بحيث تم حساب عدة عوامل وهي عامل التضاعف الفعّال (k_{eff}) والمفاعلية الفائضة ومقدار فعالية التحكم وهامش التوقيف ووجدت كما هو مبين بالجدول التالي:

	IRT-2M	IRT-4M	IRT-MR
k_{eff}	1.20665	1.21190	1.23271
$\rho_{ex} (\Delta k / k\%)$	17.1	17.5	18.9
Total worth	26.81	24.05	21.54
$\rho_{sm} (\%)$	9.7	6.6	2.6

كما تم الحصول على توزيع الفيض النيوتروني الحراري والسريع قطريا ورأسياً وأفقياً ويلاحظ النقصان الواضح للفيض الحراري في كل من القلب والبريليوم العاكس حيث توجد أنابيب التشعيع في حالة استخدام الوقود من نوع IRT-4M مما سيؤثر سلبيا في عملية تشعيع العينات ويتطلب رفع القدرة بالمقارنة بالوقود IRT-2M وكذلك تم الحصول على التوزيع الأفقي والرأسي للقدرة في أسخن أنبوب وبالتالي تحديد أسخن نقطة فيها. القدرة المنتجة في أسخن أنابيب هي 0.69 و 0.71 و 0.72 ميجا وات على الترتيب. تعتبر هذه النتائج أساسية لإجراء الحسابات الهيدروليكية وحسابات الأمان.

ABSTRACT

The Monte Carlo method is used for the comparison of the neutronic analysis of the IRT fuels. The effective multiplication factor (k_{eff}), excess reactivity, control worth, and shutdown margin are calculated and are found to be as in the following Table:

	IRT-2M	IRT-4M	IRT-MR
k_{eff}	1.20665	1.21190	1.23271
$\rho_{ex} (\Delta k / k\%)$	17.1	17.5	18.9
Total worth	26.81	24.05	21.54
$\rho_{sm} (\%)$	9.7	6.6	2.6

Also, the radial, axial, horizontal (cross sectional) thermal and fast flux distributions are obtained. When the IRT-4M fuel is used the thermal flux is reduced significantly in the core and the beryllium reflector where the irradiation channels are located. This will have an adverse effect on the irradiation of samples which may require power increase as compared to the IRT-2M fuel. The power distribution horizontally and axially in the hottest tube and hence the hottest spot are determined. The power produced in the hottest tubes in the three cores are 0.69, 0.71, 0.72 Mega watts respectively. These results are basic for further thermal hydraulic and safety calculations.

KEYWORDS: reactor; flux; enriched fuel; monte carlo; core; reactivity; power

INTRODUCTION

The Reduced Enrichment for Research and Test Reactors (RERTR) program was established in 1978. Its mission was to develop a substitute proliferation resistant fuel of higher-density. Low Enriched Uranium (LEU) containing less than 20 percent uranium-235 provides an isotopic barrier to nuclear weapons usability. Fuels based on the dispersion of UO_2 and UMo alloys in aluminum should meet all the main non-proliferation goals of the RERTR program with favorable implications for the reactor performance and research productivity. As the substitute fuels are developed, existing reactors would be converted to LEU and new reactors would be designed to use LEU.

The process of core conversion from highly enriched fuel to a low enriched one is usually done by preserving the structural integrity and design of the core base. Therefore, it is necessary to design fuel assemblies with the same dimensions as that of the old fuel. Elgammudi [1] used WIMSD code for the IRT fuel conversion analysis, however too many approximations were involved and results lacked important details. In this paper, the results of the Monte Carlo code MCNP [2] are presented. It has been used to simulate neutron transport in three fuel types. Low enriched uranium as UO_2 and UMo alloys dispersed in aluminum form the bases for new fuel options. Results of the simulation are compared with those of the old fuel. The most important parameters which are investigated and compared in this study include the infinite multiplication factor (k_∞), excess reactivity, control rod worth, cross sections ($\nu\Sigma_f, \Sigma_a$), radial thermal, fast flux and power density distribution in the core, axial thermal and fast fluxes and power density distribution in the hot channel.

FUEL ARRANGEMENTS AND DESCRIPTIONS [4]

Old fuel (IRT-2M)

The IRT-2M type fuel assemblies with three and four concentric tube fuel elements are shown in Figure (1).

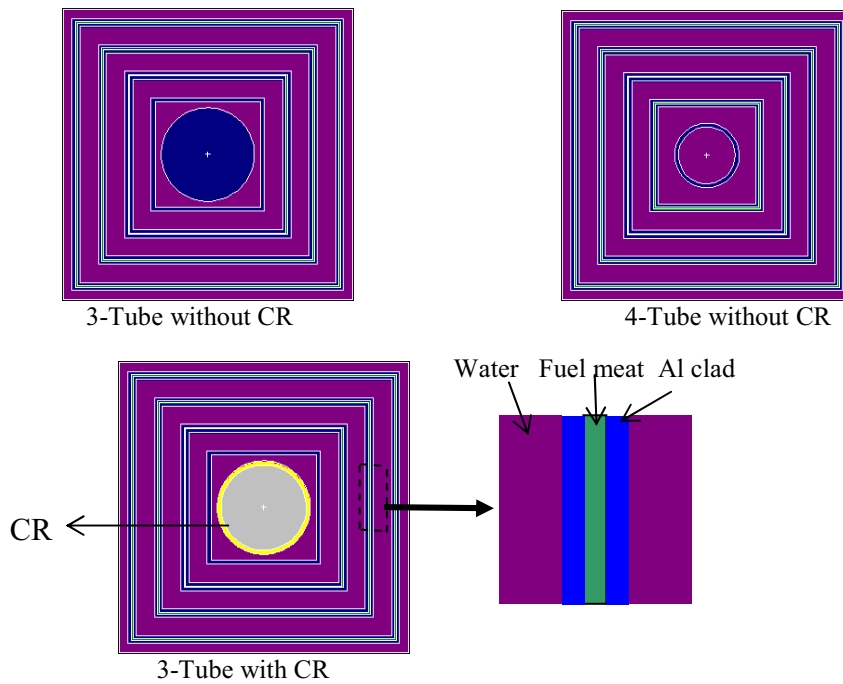


Figure 1: the old fuel (IRT-2M) assemblies

The fuel material is U-Al and the cladding is an Aluminum alloy. The core is a square lattice of 6×6 cells placed in a stationary beryllium as shown in Figure (2).

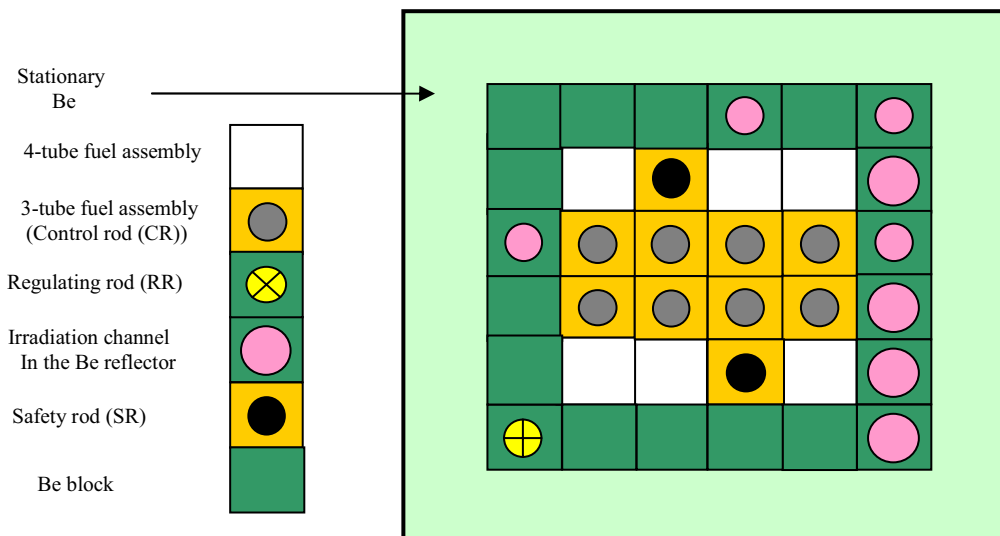


Figure 2: The reactor core layout

There are a total of 11 control rods (CR) in the core: Eight shim rods (SR) for burnup compensation, two safety rods (SR) for emergency purposes, one regulation rod (RR) for fine control.

New fuel assemblies (IRT-4M):

The IRT-4M fuel assemblies are of six or eight concentric tube fuel elements as shown in Figure (3). Fuel material is UO_2 -Al in Al cladding.

New fuels (IRT-MR) or (IRT-UMo):

IRT-MR fuel assemblies with 132 and 196 concentric pin fuel elements are shown in Figure (4). The fuel material is UMo-Al in Al cladding as shown in Figure (5).

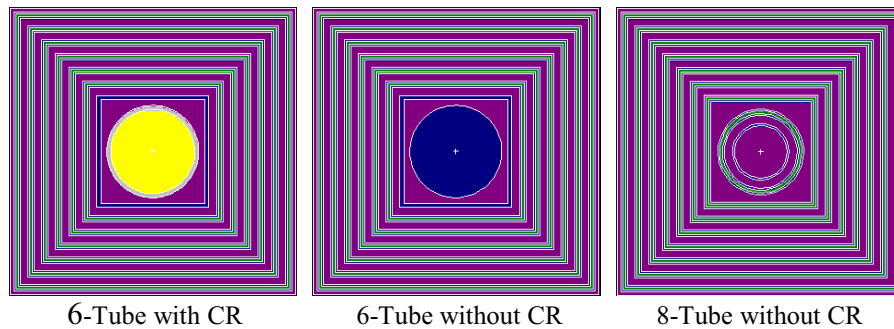


Figure 3: The new fuel (IRT-4M) assemblies

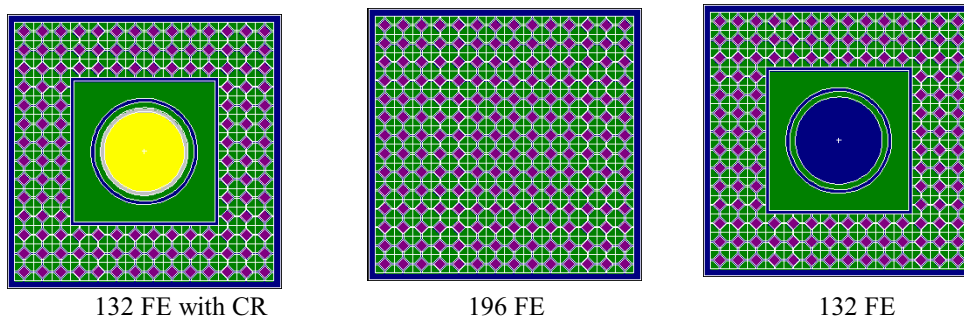


Figure 4: IRT-MR fuel

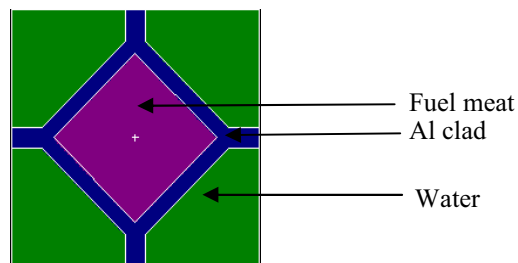


Figure 5: The IRT-MR fuel element

FUEL ASSEMBLY CALCULATIONS

The advantage of Monte Carlo calculations is the ability to account for details in geometry and material composition in three dimensions. Cross sections are read directly from ENDFB/5 files. It is considered as the most suitable of all methods for the type of calculations projected in this study since the different types of fuel assemblies considered are very much heterogeneous.

The infinite multiplication factor (k_{∞}) and two group (fast and thermal cross sections with energy boundary of 0.625 eV (Table (1)) are calculated. The assemblies with a larger number of tubes or elements maintain a higher fissile density leading to an increased multiplication and hence a higher k_{∞} .

Generally speaking, k_{∞} for all fuels are not far apart. It is also noted that $\nu\Sigma_f$ for 6/8-tube (IRT-4M) is greater than that of the 3/4-tube (IRT-2M) old fuel elements in spite of the fact that the ^{235}U enrichment of the old fuel is about four times that of the new one. This can be explained from the density ratio of 1.7 as given in Table (2) which

is quite close to the $\nu\Sigma_f$ ratio: $\frac{\nu\Sigma_f^{8\text{-tube}}}{\nu\Sigma_f^{4\text{-tube}}} = 1.54$. Consequently, an increase in fuel

density is required when a HEU fuel is to be replaced by a LEU fuel and the old core base is left unchanged.

Table 1: Macroscopic cross sections and the infinite multiplication factor for different types of fuel assemblies

		IRT-2M		IRT-4M		IRT-MR	
		3 tube	4 tube	6 tube	8 tube	132 Fuel Elements	196 Fuel Elements
$\nu\Sigma_f$	fast	3.0E-3	3.7E-3	5.5E-3	6.2E-3	3.4E-3	3.9E-3
	thermal	12.76E-2	15.00E-2	20.08E-2	23.13E-2	11.33E-2	13.11E-2
Σ_a	fast	2.5E-3	2.9E-3	5.7E-3	6.4E-3	3.4E-3	3.8E-3
	thermal	7.64E-2	8.74E-2	11.05E-2	12.56E-2	6.86E-2	7.63E-2
k_{∞}		1.63562	1.67774	1.64399	1.65989	1.64965	1.65516

Table 2: Density ratio between 8 and 4-tube fuel assemblies (TFA)

	V_{tube} (cm ³)	$M_{u^{235}}$ (grams)	$\rho_{^{235}\text{U}}$ $\left(\frac{\text{g}}{\text{cm}^3}\right)$	density ratio
4-TFA	2965.105	183.813	0.062	1.7
8-TFA	3067.35	318.310	0.104	

CORE CALCULATIONS

Complete core configuration is used in order to compute the effective multiplication factor (k_{eff}), control elements worth, radial and axial flux, and power profiles. The core loaded with fresh fuel and its reflectors are described in detail to the code. Figure (6) shows the horizontal and vertical views of the core drawn by the code as described in the input file.

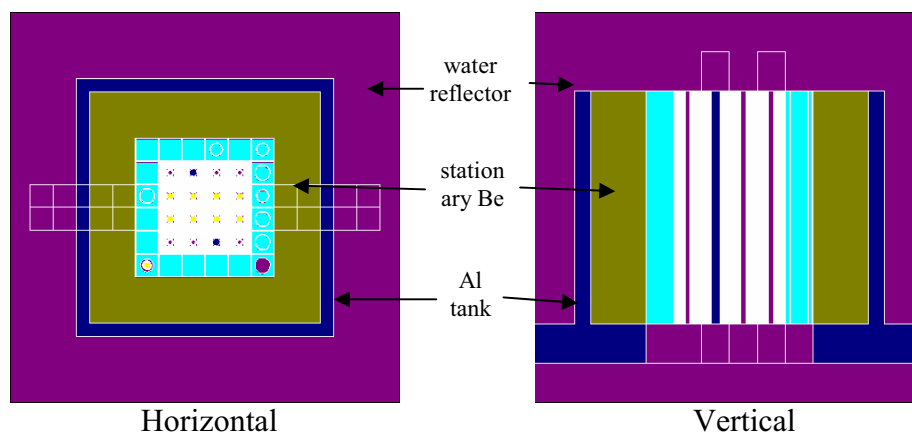


Figure 6: Radial and axial views of the reflected core

EFFECTIVE MULTIPLICATION FACTOR CALCULATIONS

Criticality calculation at the beginning of life (BOL) for a clean core is carried out using different control element settings. Referring to appendix, the fuel density of the type UMo-Al is the highest, followed by the IRT-4M and finally the IRT-2M. This explains the variation in both the effective multiplication factor (k_{eff}) (Table (3)) and the excess reactivity (Table (4)). The worth defined as: $\Delta\rho = \rho_{rods-out} - \rho_{rods-in}$ is given in Table (4).

The higher total worth of the old fuel control elements makes the shut down margin: $\rho_{sm} = \Delta\rho_t - \rho_{ex}$ higher as well. The worth of control elements in the IRT-MR core is the least implying reconsideration of control element design.

Table 3: The multiplication factor at BOL

	k_{eff}		
	IRT-2M	IRT-4M	IRT-MR
All CR+2-SR+RR out	1.20665	1.21190	1.23271
RR in	1.20364	1.20634	1.22725
2SR in	1.14853	1.15679	1.18160
4 inner CR in	1.07315	1.09192	1.12137
4 outer CR in	1.09871	1.10818	1.13603
All CR+2SR+RR in	0.91175	0.93840	0.97409

Table 4: Reactivity parameters

	IRT-2M	IRT-4M	IRT-MR
$\rho_{ex} (\Delta k / k\%)$	17.1	17.5	18.9
1-R.R	0.207	0.380	0.361
2-S.R	4.194	3.931	3.509
4-C.R inner	10.310	9.067	8.055
4-C.R outer	8.142	7.723	6.904
Total worth	26.81	24.05	21.54
$\rho_{sm} (\%)$	9.7	6.6	2.6

FLUX DISTRIBUTION

In Monte Carlo calculations particles move around randomly in tracks and the output is designated by the user according to demand. For instance, if the thermal and fast flux distributions are wanted, three dimensional cells and two energy bins are defined. Therefore, the numbers of tracks in each cell within the energy bin are counted. A series of cells in whatever orientation gives the desired distribution. Results are normalized to actual values using the total power. The fast and thermal fluxes in units of n/cm^2 -sec are calculated in all fuel assembly cells, and additional cells in the removable and stationary beryllium, Aluminum and water. The horizontal distributions of the fast and thermal fluxes are presented in Tables (5), (6), and (7) for the three fuel types based on Figure (7).

Table 5: Thermal and fast horizontal flux distributions (IRT-2M)($\times 10^{14}$)

					1.83	1.49	1.45	1.55	1.45	1.82					
					1.56	3.02	3.18	3.51	2.96	1.46					
Th.04	.18	.20	.82	1.69	2.10	1.46	1.51	1.47	1.43	2.02	1.61	.78	.19	.18	.04
F.002	.01	.03	.15	0.60	1.85	3.13	3.63	3.59	3.07	1.79	0.57	.15	.03	.02	.002
Th.04	.18	.19	.82	1.67	2.01	1.45	1.49	1.48	1.42	2.01	1.61	.77	.19	.17	.04
F.003	.02	.03	.16	0.62	1.91	3.14	3.63	3.60	3.05	1.77	0.56	.15	.03	.01	.002
					1.77	1.48	1.55	1.44	1.43	1.81					
					1.50	1.01	3.48	3.13	2.90	1.40					

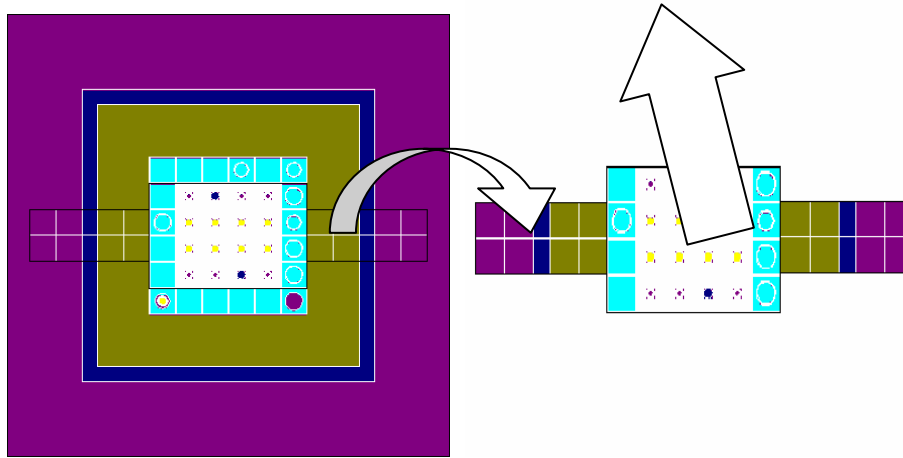


Figure 7: Horizontal view of the core

Table 6: Thermal and fast horizontal flux distributions (IRT-4M)($\times 10^{14}$)

					1.57	0.84	0.78	0.81	0.82	1.59					
					1.82	3.42	3.53	3.84	3.36	1.72					
Th.04	.19	.20	.82	1.61	1.74	0.78	0.73	0.72	0.76	1.73	1.58	.79	.19	.18	.04
F.002	.02	.03	.18	0.71	2.14	3.51	3.87	3.86	3.44	2.07	0.65	.17	.03	.02	.002
Th.04	.19	.20	.81	1.59	1.65	0.78	0.73	0.72	0.75	1.69	1.56	.77	.19	.18	.04
F.002	.02	.03	.18	0.70	2.21	3.50	3.88	3.83	3.40	2.02	0.64	.16	.03	.02	.003
					1.54	0.82	0.80	0.75	0.79	1.54					
					1.78	3.36	3.78	3.43	3.24	1.63					

Table 7: Thermal and fast horizontal flux distributions (IRT-MR) ($\times 10^{14}$)

					1.51	0.74	0.60	0.73	0.72	1.54					
					1.82	3.38	2.64	3.78	3.35	1.71					
Th.04	.18	.20	.80	1.59	1.68	0.61	0.58	0.58	0.60	1.66	1.56	.79	.19	.17	.03
F.002	.01	.03	.18	0.67	2.08	2.63	2.92	2.91	2.60	2.05	0.66	.16	.03	.02	.002
Th.04	.18	.20	.81	1.57	1.61	0.61	0.57	0.58	0.59	1.62	1.49	.78	.19	.18	.03
F.002	.01	.03	.17	0.68	2.14	2.62	2.91	2.91	2.57	1.99	0.65	.17	.03	.02	.002
					1.43	0.71	0.70	0.58	0.72	1.49					
					1.77	3.29	3.73	2.60	3.26	1.62					

The radial thermal flux distributions for all fuel types are shown in Figure (8). The old fuel has the highest thermal flux in the core and in the removable Be. It is attributed to the rather strong moderating effect of the larger water content of the old fuel assemblies. This same effect causes the radial fast flux in the old core to be lower than that in the new core as shown in Figure (9). The axial thermal and fast flux distributions are shown in Figures (10) and (11) respectively. The peaking of the thermal flux in the old fuel is also due to strong moderation.

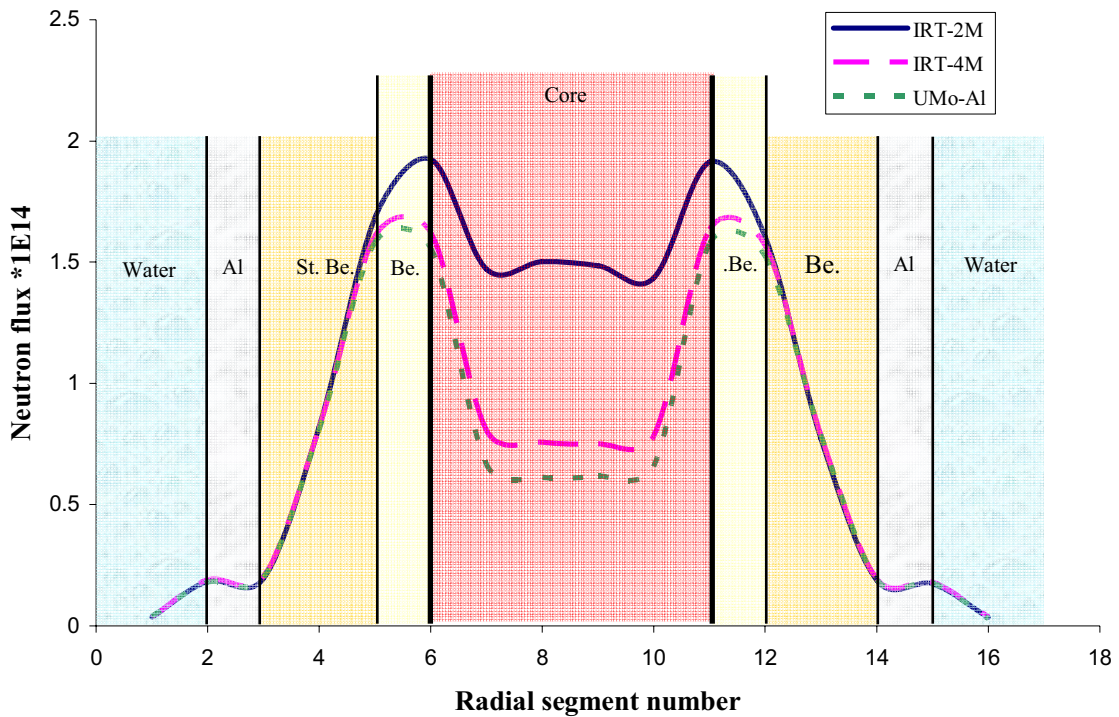


Figure 8: Radial thermal flux distribution for all types of fuel

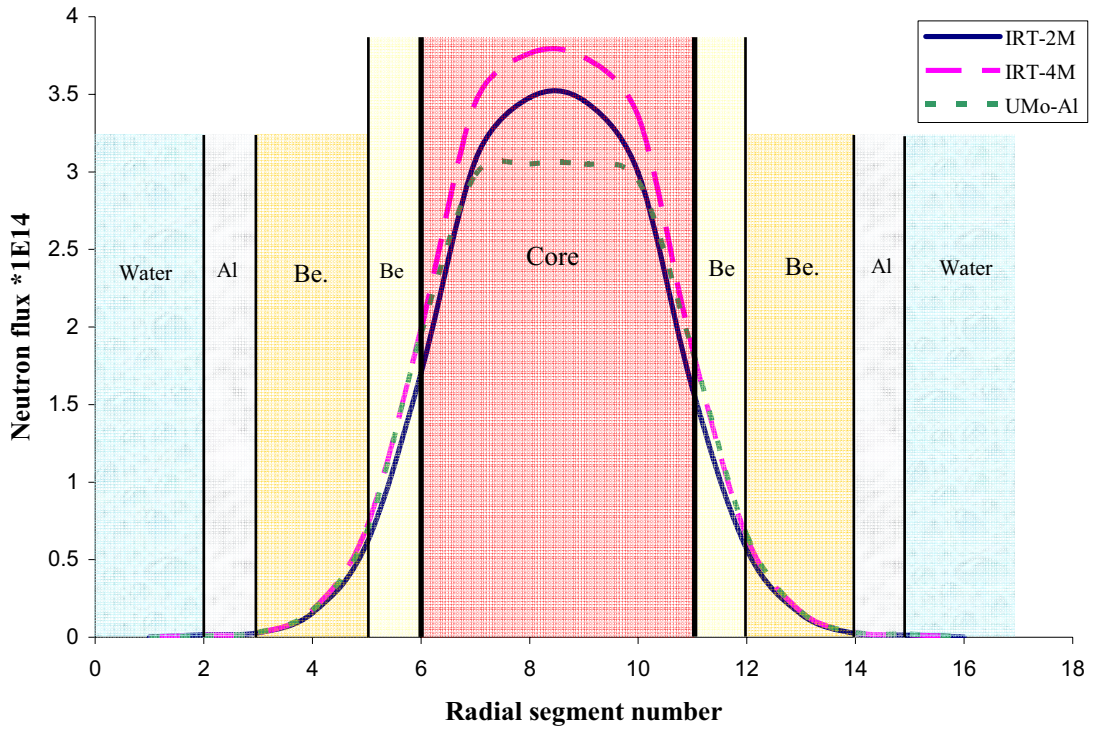


Figure 9: Radial fast flux distribution for all types of fuel

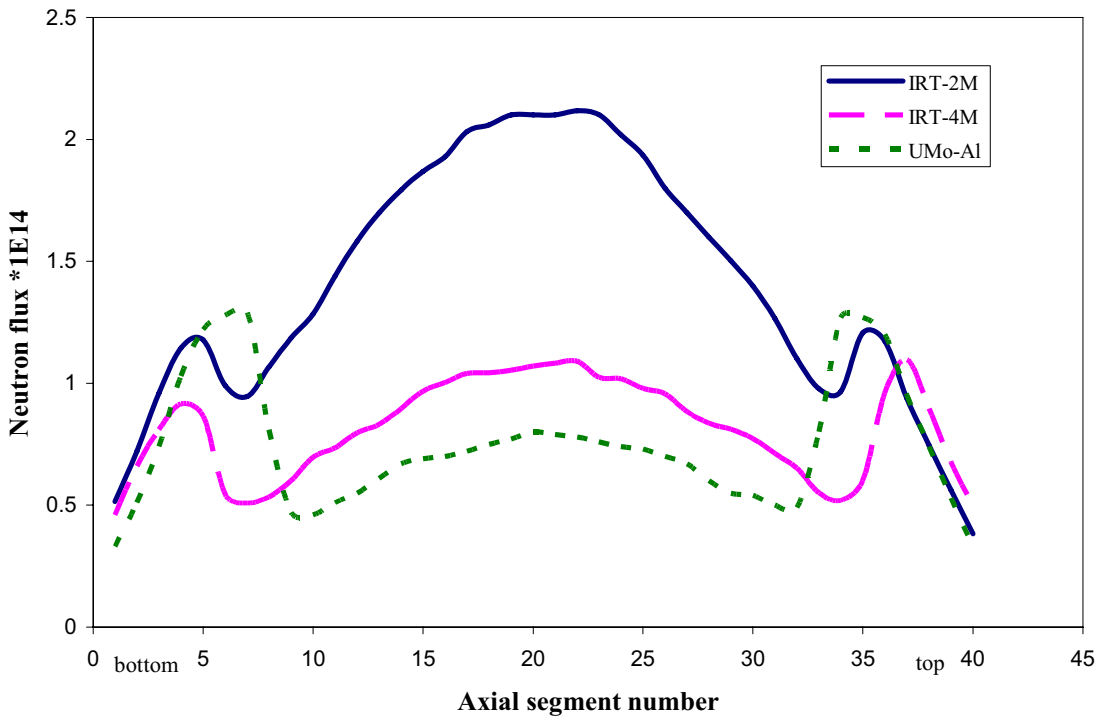


Figure 10: Axial thermal flux distribution for all types of fuel

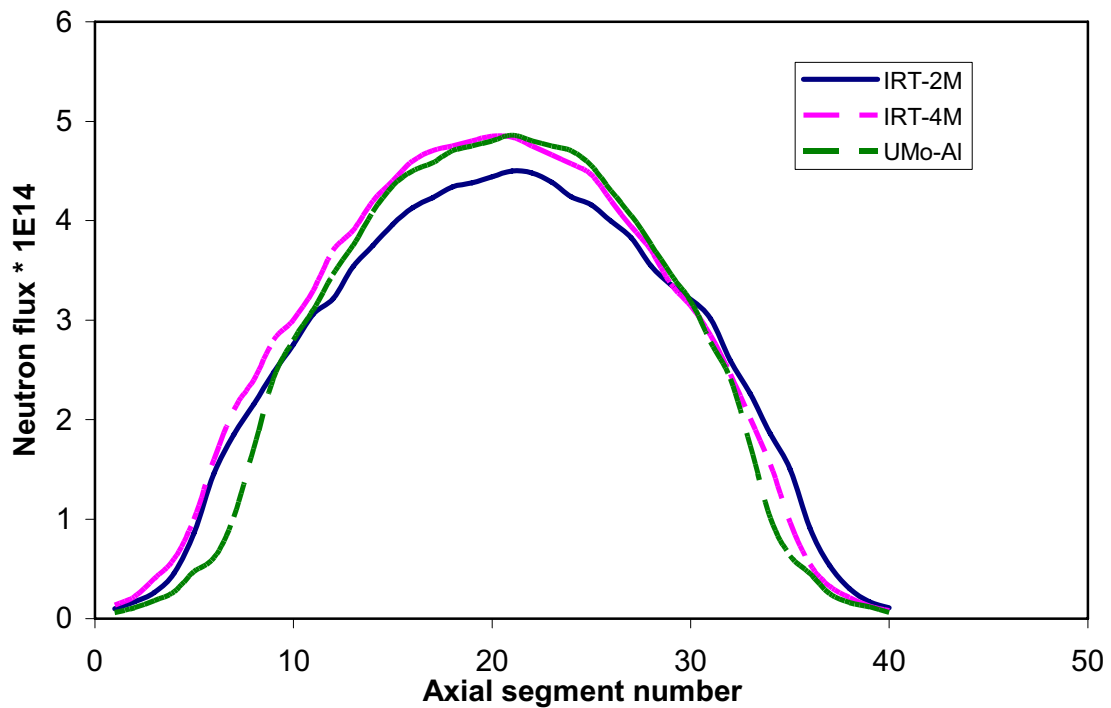


Figure 11: Axial fast flux distribution for all types of fuel

POWER DISTRIBUTIONS

The power produced in every tube assembly for the three fuel types is calculated on the basis of maximum reactor power of 10 Mega watts. Table 8 shows the power produced in every tube assembly of the four by four tube cores. It is nearly uniform. The highest power produced is 0.69 Mw in tube position 1-3 of the IRT-2M fuel. On the other hand, the highest power produced in the IRT-4M fuel is 0.71 Mw and in the UMo-AI fuel is 0.72 Mw and both are in tube 1-1. These are the hottest tubes.

Table 8: Power in Mw produced in the 4 by 4 tube positions

		1	2	3	4
IRT-2M IRT-4M UMo-AI	1	0.67 <u>0.71</u>	0.60 0.61	<u>0.69</u> 0.67	0.65 0.70
	2	0.60 0.60	0.62 0.57	0.60 0.56	0.59 0.61
	3	0.60 0.62	0.61 0.56	0.60 0.56	0.59 0.60
IRT-2M IRT-4M UMo-AI	4	0.66 0.70	0.68 0.66	0.60 0.60	0.64 0.67
		0.70	0.67	0.58	0.70

Figure (12) shows the axial power distribution in such tubes which is nearly sinusoidal and similar in all types of fuel. The hottest spot is at a height of 16 cm in all kinds of hot tubes. The results are essential for carrying out thermal hydraulics calculations which are necessary for safety analysis

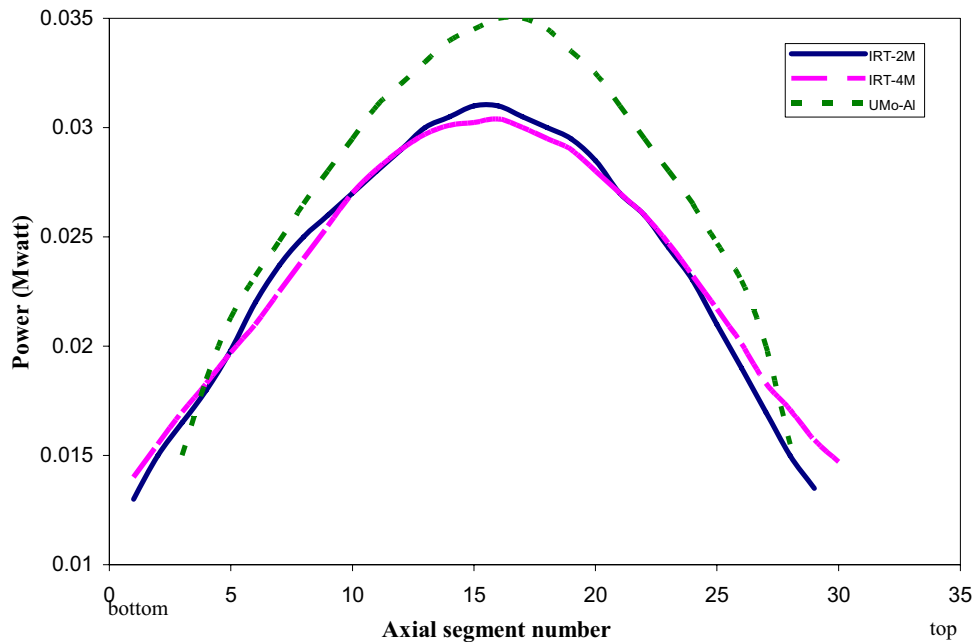


Figure 12: Axial power distribution in the hottest tubes for all types of fuel

CONCLUSION

The transformation from HEU to LEU core is achieved by increasing fuel density and increasing the number of tubes per fuel assembly leaving less space for water. Therefore, the moderating power is decreased leading to a remarkable reduction in the thermal flux which will have an effect on the irradiation of samples. Its effect on cooling or accommodation for swelling needs to be investigated. The values listed in the appendix for the ^{235}U enrichment and the fuel densities allow reasonable excess reactivity and shut down margin. The control elements worth in the IRT-4M core is nearly the same as in the old core. On the other hand, the control elements worth in the UMo-MR fueled core is low and may not be controlled with the same number of control elements, or the control element design should be reconsidered. In conclusion, the IRT-4M fuel exhibits inferior characteristics as compared to the IRT-2M fuel. The later had been used in the old core of the Tajura research reactor and the IRT-4M fuel has just been loaded in the new core and went critical during the writing of this paper.

REFERENCES

- [1] El-Gammudi. Feasibility study of core conversion from HEU to LEU IRT Fuel using WIMSD code, B.Sc project, nuclear Engineering department, Alfateh University, Tripoli, Libya, 2004.
- [2] J.Briesmeister, MCNP-4C code manual, 2004
- [3] C.D. Harmon, R.D. Busch, J.F. Briesmeister, R.A. Forster, and T.Goorley. Criticality Calculations with MCNP5: A Primer, 2004.

- [4] A.V. Vatulin, Y.A. Stetskiy, V.A. Mishunin, V.B. Suprun, and I.V. Dobrikova. Development of new-type fuel elements for Russian-built Research Reactors, 2001.
- [5] J.E. Matos, Accelerating the Design and Testing of LEU Fuel Assemblies for Conversion of Russian-Designed Research Reactors Outside Russia
- [6] International Meeting on Reduced Enrichment for Research and Test Reactors, October 5-10, 2003, Chicago, IL USA

Appendix: fuel assembly data for the three fuels

	IRT-2M	IRT-4M	IRT-MR
²³⁵ U enrichment , wt%	80	19.7	19.7
No. of fuel tubes Per assembly	3/4	6/8	132/196 elements
No. of Assemblies In Core	3/4tube: 10/6	6/8tube : 10/6	132/196elem: 10/6
Ass. cross Section , cm x cm	7.15×7.15	7.15×7.15	7.15×7.15
²³⁵ U mass, g	3/4tube: 190/162.8	6/8tube :265/300	132/196elem: 345.84/513.52
Fuel meat composition	37%U-63%Al	62.2%UO ₂ -37.8%Al	68.09%U-7.47% Mo-24.44Al
Active Fuel Length , cm	58	60	50
Cladding Material	Al Alloy	Al Alloy	Al Alloy
Cladding thickness , cm	0.08		
Fuel material	U-Al	UO ₂ -Al	UMo
(Meat/Clad/tube)	0.04/0.08/0.2	0.07/0.045/0.16	0.2263/0.04/0.485
Thickness , cm			
Fuel density , gm/cm ³	3.8	4.97	7.5